

Biodegradation Performance of Magnesium Matrix Composite as a Biomedical Implant

Kun Yu^{1,2*}, Yilong Dai^{1,2}, Yu Zhang¹, Tao Zhang², Fang Hongjie², Liangjian Chen³

1. School of Materials Science and Engineering, Central South University, Changsha 410083
2. Department of Materials Science and Engineering, Yantai Nanshan University, Yantai 265700, China
3. XiangYa Third Hospital, Central South University, Changsha 410083

*Corresponding author

School of Materials Science and Engineering, Central South University, Changsha 410083

Tel: 86-731-88879341

Fax: 86-731-88876692

e-mail: yukun2010@csu.edu.cn

Abstract

A Mg-Zn-Tricalcium Phosphate composite with a chitosan coating was prepared in this investigation to study its biodegradation performance both *in vitro* and *in vivo* conditions. The immersion corrosion rate of the chitosan coated composite is lower than that of the uncoated composite in simulated body fluid. The *in vitro* cytotoxicity test shows that the chitosan coated specimens is safe for cellular applications. When the chitosan coated composite is tested *in vivo*, the concentration of metal ions from the composite observed in the venous blood of Zelanian rabbits is less than the uncoated composite specimens. The chitosan coating slows down the *in vivo* degradation of the composite after surgery. *In vivo* testing also indicates that the chitosan coated composite is harmless to important visceral organs, including the heart, kidneys and liver of the rabbits. The new bone formation surrounding the chitosan coated composite implant shows that the composite improves the concrecence of the bone tissues.

Key words: Biodegradation; Magnesium matrix composite; Chitosan coating; Implant

1. Introduction

Magnesium alloys have the potential to serve as biomedical implants because their elastic modulus matches that of cortical bone tissue, allowing them to avoid the stress shielding effect induced by a serious mismatch between the modulus of the natural bone and implants [1][2]. Mg-based implants corrode when in contact with body fluid, where the degradation occurs via corrosion in the electrolytic physiological environment [3][4]. Therefore, magnesium alloys are candidates for biodegradable implants for repairing bone fractures [5]. Biodegradable magnesium alloys can provide good mechanical properties and produce non-toxic corrosion products in physiological systems [6][7]. However, some disadvantages to the biodegradation of magnesium alloys are perceived, including a rapid corrosion rate, hydrogen gas emissions and a high environmental pH value [5][8]. Since rapid corrosion is an intrinsic response of magnesium to the human body's fluid or plasma, controlling or decreasing the corrosion rate of magnesium in body fluid is a significant issue in the development of magnesium implants [9]. Alloying can significantly slow down the corrosion rate of magnesium in body fluids. For example, magnesium alloyed with Al, or AZ series magnesium alloys, can reduce dissolution and hydrogen evolution rates [10]. But the presence of Al ions in the human body is undesirable for human health. Including other alloying elements in the magnesium matrix such as cadmium, manganese or rare earth metals has also been proposed in order to improve the alloy's corrosion resistance, but these elements can barely be tolerated because they are poisonous to the human body [11~13]. Therefore, there is a limited number of elements that may be employed in magnesium alloys used for biomaterials.

One of the alternatives for adjustment of the corrosion rates of Magnesium alloys to meet the requirements of bone repair is the application of Mg-based metal matrix composites (MMCs) and their surface coating treatments [14][15]. Previous studies show that Mg-6%Zn-10%Ca₃(PO₄)₂ exhibits good synthetic properties as a biomaterial implant [16]. A suitable addition of hydroxyapatite or tricalcium phosphate can decrease the corrosion rate of the magnesium matrix and increase its biocompatibility. An anodizing or micro-arc oxidizing surface treatment of Magnesium alloys has been reported to improve their corrosion resistance. Such surface treatments of magnesium alloys have been employed for industrial applications but have seldom been explored for use in a bio-environment [17~19]. The surface treatment of the implanted magnesium must be non-toxic to the human body. Chitosan has been proven to be biocompatible with the human body [20]. Therefore, in the present investigation, a chitosan coatings is applied to the surface of an experimental Mg-6%Zn-10%Ca₃(PO₄)₂ composite in order to adjust its biodegradable behavior and to study the effects of the chitosan coating on the *in vitro* and *in vivo* corrosion characteristics of the magnesium implant.

2. Materials and methods

2.1 Material production and measurement

The experimental composite specimens were prepared with Mg, Zn and $\text{Ca}_3(\text{PO}_4)_2$ powders and sintered at 620~640 °C for 1 hour in a vacuum furnace under argon gas protection. The average particle diameter of the Mg and Zn powders was 23.0 μm , and the average particle diameter of the $\text{Ca}_3(\text{PO}_4)_2$ powder was 7.85 μm . The specimens for testing were cut from the sintered composite billets. The specimens for chitosan coating were first abraded using sand paper and treated with a 40% $\text{H}_3\text{PO}_4+\text{H}_2\text{O}$ solution as a pre-treatment. Chitosan, with a molecular weight of 300kDa, was mixed in a 0.2% acetic acid solution to form the coating mixture. The coating mixture was then smeared on the surface of the composite specimens and solidified at 60 °C for 30 minutes. All of the experimental results for *in vitro* corrosion testing and *in vivo* measurements were obtained from the chitosan coated composite specimens. The uncoated Mg-6%Zn-10% $\text{Ca}_3(\text{PO}_4)_2$ composite was utilized experimentally as the control specimen. The microstructures of the experimental MMCs were observed with a JEOL JSM-5600Lv scanning electron microscope (SEM) with an energy-dispersive X-ray spectroscope (EDX).

2.2 In vitro corrosion testing

The *in vitro* corrosion test was performed in static simulated body fluid (SBF) at 37 ± 0.2 °C for 30 days. The SBF was a solution of recently boiled distilled water containing 8.6 g of sodium chloride, 0.3 g of potassium chloride, and 0.33 g of calcium chloride per liter. The SBF was not stirred during the experiments and was saturated with atmospheric oxygen. The SBF temperature was controlled by an HTW-10B water bath kettle. The change in the pH values of the SBF after corrosion testing was determined using a Mettler Toledo FE20-pH sensor.

2.3 Cytocompatibility assessments

The cytotoxicity of the experimental composites was measured via indirect contact testing according to ISO 10993-5:1999. The composite specimens were immersed in a 10% fetal bovine serum in a humidified incubator with 95% relative humidity and 5% CO_2 at 37 °C. L-929 cells were cultured in Dulbecco's modified Eagle's medium (DMEM). The culture medium was replaced by 100% extraction media or by 50% or 10% dilutions. The DMEM acted as a negative control, and a sample of the DMEM medium containing phenol acted as a positive control. 3-(4,5-Dimethylthiazol-2-yl)-2,5-diphenyltetrazolium bromide (MTT) was then dissolved in a phosphate-buffered saline (PBS) solution at a concentration of 5 mg/ml. The samples were incubated for 4 hours after adding 10 μl of the MTT solution. Subsequently, 100 ml of the formazan solution were

added to each sample, and the optical density (OD) was measured using a spectrophotometer. The cell relative growth rate (RGR) was calculated as follows:

$$\text{RGR} = (\text{OD}_{\text{test}} / \text{OD}_{\text{negative}}) \times 100\%$$

2.4 *In vivo* biodegradation testing

All animal experiments, including anesthetic, surgical and post-operative treatments, were approved by and fulfilled the requirements of the Ethics Committee of the Xiangya 3rd Hospital and complied with the animal welfare legislation of the Chinese government. Eight adult male Zelanian rabbits weighing between 2.0 and 2.5 kg were randomly assigned to two groups. One group received uncoated Mg-6%Zn-10%Ca₃(PO₄)₂ composite implants, while the other received the chitosan coated specimens. The biodegradation performance of the magnesium composite implants in both rabbit groups were measured at the times of 2 weeks, 4 weeks, 8 weeks and 12 weeks. In the animal experiments, a 12×5×2 mm sized splint from the two types of experimental composites was fastened to the animal's pre-broken femoral shaft. A 5×5×2 mm size composite sample was implanted into the dorsal muscle of the animals. All rabbits were anaesthetized with amyl-barbiturate (30 mg/kg) for the surgery. Venous blood samples from the rabbits were phlebotomized at different times from one day to 12 weeks to detect the variations in the concentration of Mg²⁺, Zn²⁺, and Ca²⁺ ions in the blood. The animals were euthanized 12 weeks after the surgery. The muscle tissue around the implanted composite and the tissue from the heart, liver and kidneys of the rabbit were also stained with hematoxylin and eosin (HE) for histological analysis and in order to detect whether the degradation of the composites harmed these important visceral organs. Micro-computed tomography devices were used to observe the *in vivo* degradation process of the composite and the pre-broken bone healing process after the implant fixation.

3. Results

3.1. Morphology and microstructure characterization

The surface morphology of the Mg-6%Zn-10%Ca₃(PO₄)₂ composite without chitosan is shown in Fig.1(a), with the polished scratches from the sand paper clearly exhibited. The 40%H₃PO₄+H₂O solution pretreatment before smearing the chitosan produces a dispersed porous surface morphology, which is beneficial for the adherence of chitosan to the specimens (Fig.1 b). The specimen's surface with the chitosan is shown in Fig.1(c). The chitosan coating is integral and dense on the surface of the specimen.

The internal microstructure and the composition analysis of the Mg-6%Zn-10%Ca₃(PO₄)₂ composite are shown in Fig.2. The Ca₃(PO₄)₂ particles and the Mg-Zn compounds are distributed

homogeneously on the grain boundary of the Mg matrix.

3.2. Immersion test

In order to evaluate the effect of the chitosan coating on the surface corrosion properties of the Mg-6%Zn-10%Ca₃(PO₄)₂ composite, the comparison of specimens with or without the chitosan coating in SBF with a temperature of 37±0.2 °C is performed. The corrosion rate of the specimens and the pH value variation of the SBF are measured to investigate the difference in the corrosion behavior of the composite with the chitosan coating. The concentration of metal ions, including Mg²⁺, Zn²⁺ and Ca²⁺, in the SBF solutions is compared.

The corrosion rate (CR) of the specimens in SBF via the weight loss (ΔW) measurement method is calculated according to $CR = \Delta W / (A \cdot t)$, where A is the initial surface area and t is the immersion time. The corrosion rates of different specimens with different immersion times are shown in Fig. 3. It can be seen that the uncoated Mg-6%Zn-10%Ca₃(PO₄)₂ composite specimens exhibit a high corrosion rate during the first 7 days and maintain a rate approximately three times greater than the chitosan coated specimens until a time of 30 days. An obvious decrease in the corrosion rate of the chitosan coated specimens is observed, especially during the first immersion stage of 7 days, with its corrosion rate maintaining a low level during the whole immersion period.

The pH values of SBF during the immersion period also reflect the corrosion resistant affect of chitosan on the Mg-6%Zn-10%Ca₃(PO₄)₂ composite. The results can be shown in Fig.4. The pH values of SBF increase to about 9.5~10 quickly for the uncoated Mg-6%Zn-10%Ca₃(PO₄)₂ composite specimens immersed for 4 days. However, the pH values of the SBF for the chitosan coated specimens changed slightly during the first few days, consistently maintaining values of less than 8, with values of approximately 8 until the end of the 30-day period.

Such obvious corrosion behavior differences between the uncoated and chitosan coated Mg-6%Zn-10%Ca₃(PO₄)₂ composite specimens can also be observed via the surface morphology of different specimens in the SBF. The macro-morphologies of uncoated and chitosan coated specimens after 30 days of immersion are shown in Fig. 5 (a) and (b). There is a much larger degree of corrosion for the uncoated specimen than for the chitosan coated specimen. The profile surface observations by SEM are shown in Fig.5 (c) and (d). The SEM images obviously show that the corrosion penetrates into the internal region of the uncoated specimen and that the surface exhibits a jagged pattern. Conversely, the chitosan coated specimen exhibits a smooth surface pattern and impeded corrosion inside the composite.

The concentrations of typical metal ions, such as magnesium, zinc and calcium ions, released in the

SBF of uncoated and chitosan coated specimens are also compared in Fig. 6. The curves show that the concentrations of different metal ions in the SBF exhibit different behaviors. The magnesium ion concentration of the uncoated specimens is found to increase rapidly from $5.11 \times 10^{-3} \text{ mol/l}$ to $14.60 \times 10^{-3} \text{ mol/l}$ in less than 1 day, after which the concentration of magnesium ions maintains relatively stable values of approximately $15 \times 10^{-3} \text{ mol/l}$ until the end of the 30-day period. The amount of magnesium ion leached from the chitosan coated specimen is significantly less than the amount leached from the uncoated specimen. The value of the magnesium ion concentration is less than $4 \times 10^{-3} \text{ mol/l}$ after immersion for 30 days. The zinc ion concentration of the SBF with uncoated and chitosan coated specimens is maintained steadily during the whole immersion process, though the level of zinc ions in the uncoated specimen is higher than that in the coated specimen. The calcium ions show the trend of decreasing concentrations for both specimens because they precipitate easily in the SBF.

The uncoated Mg-6%Zn-10%Ca₃(PO₄)₂ composite specimens also exhibit different mechanical properties than the chitosan coated specimens after immersion in the SBF for 30 days. Fig. 7 compared the Brinell hardness and compressive strength of two such specimens. The hardness and the compressive strength of both uncoated and chitosan coated specimens are found to be similar before immersion, but both the hardness and compressive strength decrease after immersion for 30 days. The hardness of the chitosan coated specimen remains at 32.8 and the compressive strength remains approximately 236MPa after 30 days of immersion, however, the values obtained for the uncoated specimens are much lower than those of the coated specimens. Therefore, the chitosan coating aids in maintaining the mechanical properties of the Mg-6%Zn-10%Ca₃(PO₄)₂ composite in the SBF for a period of time.

3.3 Cytocompatibility test

The MTT assay is always used to determine the cytotoxicity of metal, polymer or composite materials toward mammalian cells [13]. In this investigation, L-929 cells are cultured in different immersion extracts with concentrations of 100%, 50% and 10%. The L929 cells can adhere, survive and proliferate in all three of these extracts in a cell culture system. The RGRs of the L-929 cells are shown in Fig. 8. The cells in different extracts of the coated specimens are normal and healthy and are similar to the results of the negative control. According to the ISO 10993-5:1999 standard [21], which focuses on cytocompatibility and quantifies the toxicity level of implants, the RGRs of the cells in the extracts of the coated specimens all exceed 100%, with values of 128.3, 109.6 and 105.9, which means that the cytotoxicity of these extracts is level 0, no toxicity. Similarly, the RGRs of the cells in the extracts of the uncoated specimens display no toxicity, with RGR values of 112.8, 96.9 and 90.9. But the extracts with

50% and 100% concentrations of composites reach a level of 1 (RGR range from 75~100). Obviously, the chitosan coating improves the cytocompatibility of the Mg-6%Zn-10%Ca₃(PO₄)₂ composite.

3.4 *In vivo* test

The concentrations of different metal ions of the uncoated and chitosan coated Mg-6%Zn-10%Ca₃(PO₄)₂ composites in the venous blood of Zelanian rabbits are measured and the results are compared in Fig. 9. It has been found that the concentrations of Mg²⁺, Zn²⁺ and Ca²⁺ ions change during the experimental time. They reach maximum values between 15 days and 4 weeks, then decrease to preoperative levels after 12 weeks. The results show that the concentration of the three metal ions of the coated Mg-6%Zn-10%Ca₃(PO₄)₂ composite are less than that of uncoated composite specimens during the whole experimental period. This result indicates that the chitosan coating defers the *in vivo* degradation of the composite to after the surgery.

Fig. 10 shows the heart, liver, kidney and muscle tissues' response to the chitosan coating composite after 12 weeks of implantation. The tissues are normal, which indicates that the chitosan coating composite is harmless to these important visceral organs, similar to biological magnesium.

The implanted composite with the chitosan coating is shown in Fig. 11(a), with the micro-CT graphs of the bone fractures and the implanted composite 2 weeks after surgery are shown in Fig. 11(b). The chitosan coating stimulates the new bone tissues, which are obviously depositing and surrounding the implant. The edges of the composite implant still remain distinct, which means that the degradation of the composite is impeded by the coating. After 12 weeks, the prefabricated fracture on the bone has healed and new bone tissues around the implant can be observed. The new bone formation surrounding the implant shows that the composite improves the concrescence of the bone tissues. The composite implant visibly shows degradation, and the residual implant becomes smaller (Fig. 11 c). Throughout the entire degradation process, no obvious inflammation response is observed, despite the appearance of subcutaneous bubbles, which are the product of the degradation of the composite with the body fluid.

4. Discussion

The Mg-6%Zn-10%Ca₃(PO₄)₂ composite is potentially a wonderful implant material due to its non-toxicity and biodegradation in the rabbit body in an *in vivo* experiment. However, such biodegradation characteristics are due to the corrosion performance of the Mg matrix in the body fluid or plasma, which is a chloride containing solution. In such an environment, Mg will corrode rapidly, resulting in corrosion products, such as gas bubbles, which would influence the healing process after surgery.

With the reaction of Mg and H₂O in the body fluid, the dissolution of the Mg matrix would lead to

Mg²⁺. Mg²⁺ can be easily absorbed or consumed by the human body. Even if the amount of dissolved Mg²⁺ is in excess of the daily intake limit (300~400 mg/day), no side effects of a Mg²⁺ overdose can be found in the body [22][23]. Therefore, the dissolution of the Mg matrix in the body fluid is acceptable from a physiological point of view.

However, other corrosion products of the magnesium implant, such as gas bubbles, would harm the body [23]. Hydrogen gas bubbles, which are one of the reaction products of Mg with H₂O in the body fluid, will lead to subcutaneous bubbles and delay the healing of the surgical region. Such phenomenon are observed with the *in vivo* experiment of the Mg-6%Zn-10%Ca₃(PO₄)₂ composite implants in rabbits. Since such hydrogen gas bubbles are inevitable, the effective method to mitigate such negative effects is to reduce the release of the gas bubbles. As is well known, the low corrosion rate of a Mg implant means low rates of hydrogen evolution. This can allow the body to gradually absorb or consume such corrosion by-products and avoid the formation of subcutaneous bubbles. One of the possible solutions to such a problem is adding alloying elements to the Mg. Both zinc and Ca₃(PO₄)₂ are effective additions in the Mg matrix to improve the corrosion resistance and have been discussed in the literature [16]. However, such additions are not sufficient to impede the corrosion process. Therefore, another approach to improve the corrosion resistance of Mg is surface treatment or coating. Reference [5] provides a possible method of anodizing on the surface of Magnesium alloys to slow down the corrosion rate of Magnesium alloy. In this study, the chitosan coating is selected as another surface treatment method to prevent the corrosion of the Mg matrix because it has good biocompatibility with bone. The comparison of the hydrogen gas release of Mg-6%Zn-10%Ca₃(PO₄)₂ composite specimens in the SBF with or without chitosan coating is shown in Fig. 12. The results show that the hydrogen gas evolution volume increases quickly during the first 6 days in the immersion test for the uncoated Mg-6%Zn-10%Ca₃(PO₄)₂ composite specimen. Then the gas evolution rate decreases, so the slope of the curve becomes shallow. Such phenomenon is due to corrosion products, such as Mg(OH)₂, which can impede corrosion on the surface of specimen. The chitosan coating is an effective corrosion resistant layer to reduce the corrosion rate of the composite during the first time period. During the first 6 days, hydrogen release of the coated specimen is slowed down significantly compared to the uncoated specimen. This is helpful for the body to adjust to the composite implant and decreases the likelihood of forming subcutaneous gas bubbles.

Chitosan has the property of rapidly clotting blood and has recently gained approval in the United States and Europe for use in hemostatic agents [24]. The research found that chitosan with an average molecular weight of 700000 can stimulate bone formation in an animal model. It also found that HA

particles with a chitosan scaffold led to significant bone formation and that the tissue-engineered bone formation can use chitosan with $\text{Ca}_3(\text{PO}_4)_2$ sponges. Therefore, using chitosan to coat the surface of a Mg-6%Zn-10% $\text{Ca}_3(\text{PO}_4)_2$ composite can both improve its biocompatibility and impede the corrosion process. In this *in vivo* experiment of Zelanian rabbit broken bones, the coated chitosan stimulated bone formation during the beginning recovery period after surgery. The bone tissue slice after 4 weeks showed the capillary vessel formed in the fiber connective tissue around the implanted composite (Fig.13(a)). Some of the bone tissues formed were obvious after 8 weeks. Compared to the bone tissues with the uncoated chitosan composites [16], the chitosan coated composites stimulate the formation of bone tissues. Therefore, a suitable surface treatment with chitosan for the Mg-6%Zn-10% $\text{Ca}_3(\text{PO}_4)_2$ composite is beneficial for improved biocompatibility. Surface treatment is a shortcut to controlling the corrosion rate of the implanted magnesium alloy or composite by slowing down the hydrogen evolution. It is therefore a most promising approach that will lead to the practical application of magnesium composite implants.

5. Conclusions

- (1) Chitosan in a 0.2% acetic acid solution can be smeared on the surface of the Mg-6%Zn-10% $\text{Ca}_3(\text{PO}_4)_2$ composite and solidified at 60 °C for 30 minutes. Such chitosan coating is integral and dense on the surface of composite specimen.
- (2) The comparison of the corrosion behavior of uncoated and chitosan coated composite specimens, such as the immersion corrosion rate, the pH value variation of SBF and the different metal ions release of composite, show that the chitosan coating on the surface of the Mg-6%Zn-10% $\text{Ca}_3(\text{PO}_4)_2$ composite exhibits an obviously corrosion resistance improvement in the SBF. The chitosan coated composite specimens obtain better mechanical properties, including hardness and strength, than that of the uncoated specimens after a 30-day SBF immersion test.
- (3) A total grade of 0 for the chitosan coated specimens with an *in vitro* cytotoxicity towards L-929 cells compared with a parameter grade of 1 for the uncoated specimen indicates that such coating is safe for cellular applications.
- (4) The concentration of the metal ions of chitosan coated Mg-6%Zn-10% $\text{Ca}_3(\text{PO}_4)_2$ composite is less than that of the uncoated composite specimens in the venous blood of Zelanian rabbits during the experimental period of 12 weeks. This indicates that the chitosan coating is beneficial for slowing down the *in vivo* degradation of the composite after surgery. *In vivo* testing also indicates that the chitosan coated composite is harmless to the important visceral organs, including the heart, kidneys and liver of the rabbits.

(5) The new bone formation surrounding the chitosan coated Mg-6%Zn-10%Ca₃(PO₄)₂ composite implant shows that the composite improves the concretion of the bone tissues. Importantly, the chitosan coating is an effective corrosion resistant layer that reduces the hydrogen released by the Mg matrix corrosion. This is helpful for the body's integration with the composite implant and for reduction in the formation of subcutaneous gas bubbles.

References

1. S. Gomez, R. J. Belen, M. Kiehlbauch, and E. S. Aydil, *J. Vac. Sci. Technol. A* **22**, 606 (2004).
2. H. Lamb, *Hydrodynamics*, 6th ed. (Cambridge University Press, Cambridge, England, 1940), pp. 573, 645
- [1] B. Basu, D. Katti, A. Kumar, *Advanced Biomaterials Fundamentals, Processing and Applications*. (New Jersey: John Wiley & Sons, Inc., 2009), pp.12, 45.
- [2] M. Niinomi, *Met Mater Trans A*. **33**, 477 (2002).
- [3] B. Heublein, R. Rohde, V. Kaese, M. Niemeyer, W. Hartung, A. Haverich, *Heart*. **89**,651 (2003).
- [4] F. Witte, V. Kaese, H. Haferkamp, E. Switzer, M. A. Lindenberg, C.J. Wirth, *Biomaterials*. **26**, 3557 (2005).
- [5] G.L. Song, S. Z. Song, *Adv. Eng. Mater.* **9**, 298 (2007).
- [6] M. Wolf-Dieter, M. Lucia Nascimento, Monica Fernández Lorenzo de Mele, *Acta Biomaterialia*. **6**, 1749 (2010).
- [7] Staiger MP, Pietak AM, Huadmai J, Dias G. *Biomaterials*. **27**, 1728(2006).
- [8] N. T. Kirkland, N. Birbilis, M.P. Staiger, *Acta Biomaterialia*. **8**, 925 (2012).
- [9] F. Witte, J. Fischer, J. Nellesen, H.A. Crostack, V. Kaese, A.K. Pisch, *Biomaterials*. **27**,1013 (2006).
- [10] M. Alvarez-Lopez, M. D. Pereda, J. A. del Valle, M. F. Lorenzo, M. C. Garcia-Alonso, O. A. Ruano, *et al. Acta Biomaterialia*. **6**,1763 (2010).
- [11] H. Bourg, A. Lisle, *Biomaterials Developments and Applications*. (New York: Nova Science Publishers, Inc., 2010), pp.224, 284.
- [12] S.A. Guelcher, J.O. Hollinger. *An Introduction to Biomaterials*, (Boca Raton FL: Taylor & Francis Group, CRC press, 2006), pp.11, 74.
- [13] G. Ciapetti, E. Cenni, L. Pratelli, Pizzoferrato A. *Biomaterials*. **14**, 359 (1993).
- [14] F. Witte, F. Feyerabend, P. Maier, J. Fischer, M. Stormer, C. Blawert. *Biomaterials*. **28**, 2163(2007).
- [15] L.P. Xu, F. Pan, G.N. Yu, L. Yang, E.L. Zhang, K. Yang, *Biomaterials*. **30**, 1512 (2009).
- [16] K. Yu, L.J. Chen, J. Zhao, S.J. Li, Y.L. Dai, Q. Huang, Z.M. Yu, *Acta Biomaterialia*. **8**, 2845 (2012).
- [17] I. J. Hwang, D.Y. Hwang, Y.G. Ko, D.H. Shin. *Surface and Coatings Technology*. **206**, 3360 (2012).
- [18] Y. Zhang, K.F. Bai, Z.Y. Fu, C.L. Zhang, H. Zhou, L.G. Wang. *Applied Surface Science*. **258**, 2939 (2012).
- [19] B. Allen, Z.J. Chen, *Surface and Coatings Technology*. **203**, 1956 (2009).
- [20] S.W. Kim, M.W. Gaber, J. A. Zawaski, F. Zhang, M. Richardson, X.A. Zhang. *Biomaterials*. **27**, 4743 (2009).
- [21] J.R. Davis, *Handbook of Materials for Medical Devices*. (OH: ASM international, 2006), pp.136,181.
- [22] R. Zeng, W. Dietzel, F. Witte, N. Hort, C. Blawert, *Advanced Engineering Materials*. **10**, B3 (2008).
- [23] G.L. Song, *Corrosion Science*. **49**,1696 (2007).
- [24] M. Dash, F. Chiellini, R. M. Ottenbrite, E. Chiellini. *Progress in Polymer Science*. **36**,981 (2011).
- [25] R.A. Muzzarelli, M. Mattioli-Belmonte, C. Tietz, R. Biagini, G. Ferioli, M.A. Brunelli, *Biomaterials*. **15**, 1075 (1994).

Figure captions

Fig.1 Surface treatments of the Mg-6%Zn-10%Ca₃(PO₄)₂ composite

- (a) surface morphology of the composite before the chitosan coating;
- (b) surface morphology of the composite with a pretreatment of 40%H₃PO₄+H₂O solution;
- (c) surface morphology of the composite with the chitosan coating.

Fig.2 The internal microstructure and the composition analysis of the Mg-6%Zn-10%Ca₃(PO₄)₂ composite

- (a) Microstructure morphology of the Mg-6%Zn-10%Ca₃(PO₄)₂ composite seen by SEM;
- (b) EDX composition analysis, with point A showing the matrix;
- (c) EDX composition analysis, with point B showing the Mg-Zn compound;
- (d) EDX composition analysis, with point C showing the Ca₃(PO₄)₂ particles.

Fig.3 The corrosion rate curves of uncoated and chitosan coated specimens with immersion time

Fig.4 pH value variation of SBF solutions with immersed uncoated and chitosan coated specimens

Fig.5 Corrosion of uncoated and chitosan coated specimens immersed in SBF

The macro-morphologies of chitosan uncoated (a) and chitosan coated (b) specimens after immersing for 30 days.

The SEM observations of the corrosion penetrating into the internal region of the composite of uncoated (c) and chitosan coated (d) specimen.

Fig.6 Concentrations of magnesium ions (a), zinc ions (b) and calcium ions (c) released in the SBF

Fig.7 Different mechanical properties of the uncoated and chitosan coated specimens after immersion in the SBF for 30 days

Fig.8 RGRs of the L-929 cells cultured in different extracts of uncoated and chitosan coated composites, P>0.05

Fig.9 Concentration of (a) magnesium ions, (b) zinc ions and (c) calcium ions from the uncoated and chitosan coated composites in the venous blood of Zelanian rabbits

Fig.10 Hematoxylin and eosin (HE) stained slices of (a) heart, (b) liver, (c) kidney and (d) muscle tissues

Fig.11 Implanted composite with chitosan coating

- (a) Surgery of the chitosan coated composite with the rabbit
- (b) The bone fractures and the implanted composite after surgery 2 weeks;
- (c) The degraded composite and the new formed bone tissues after 12 weeks.

Fig.12 Hydrogen evolution compared with the chitosan coated and uncoated specimens

Fig.13 Bone tissue slices after (a) 4 weeks and (b) 8 weeks around the implanted composite

Fig.1

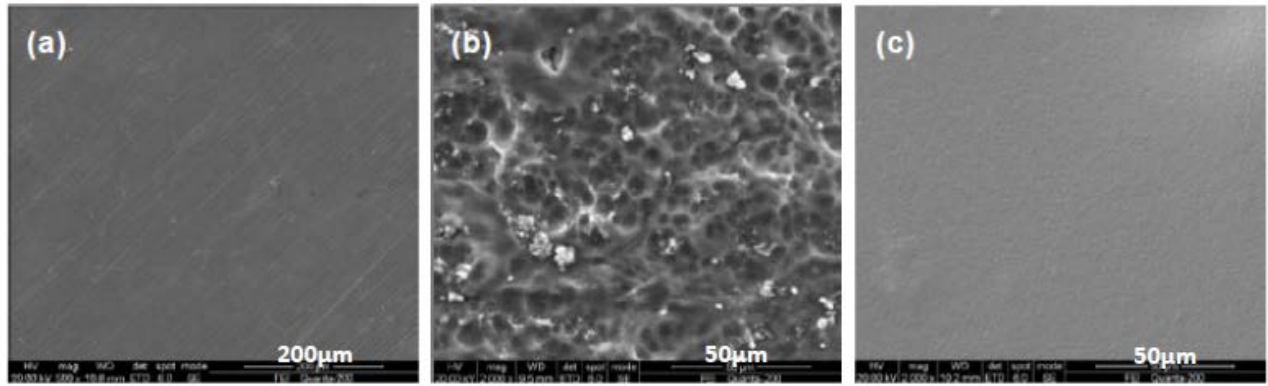


Fig.2

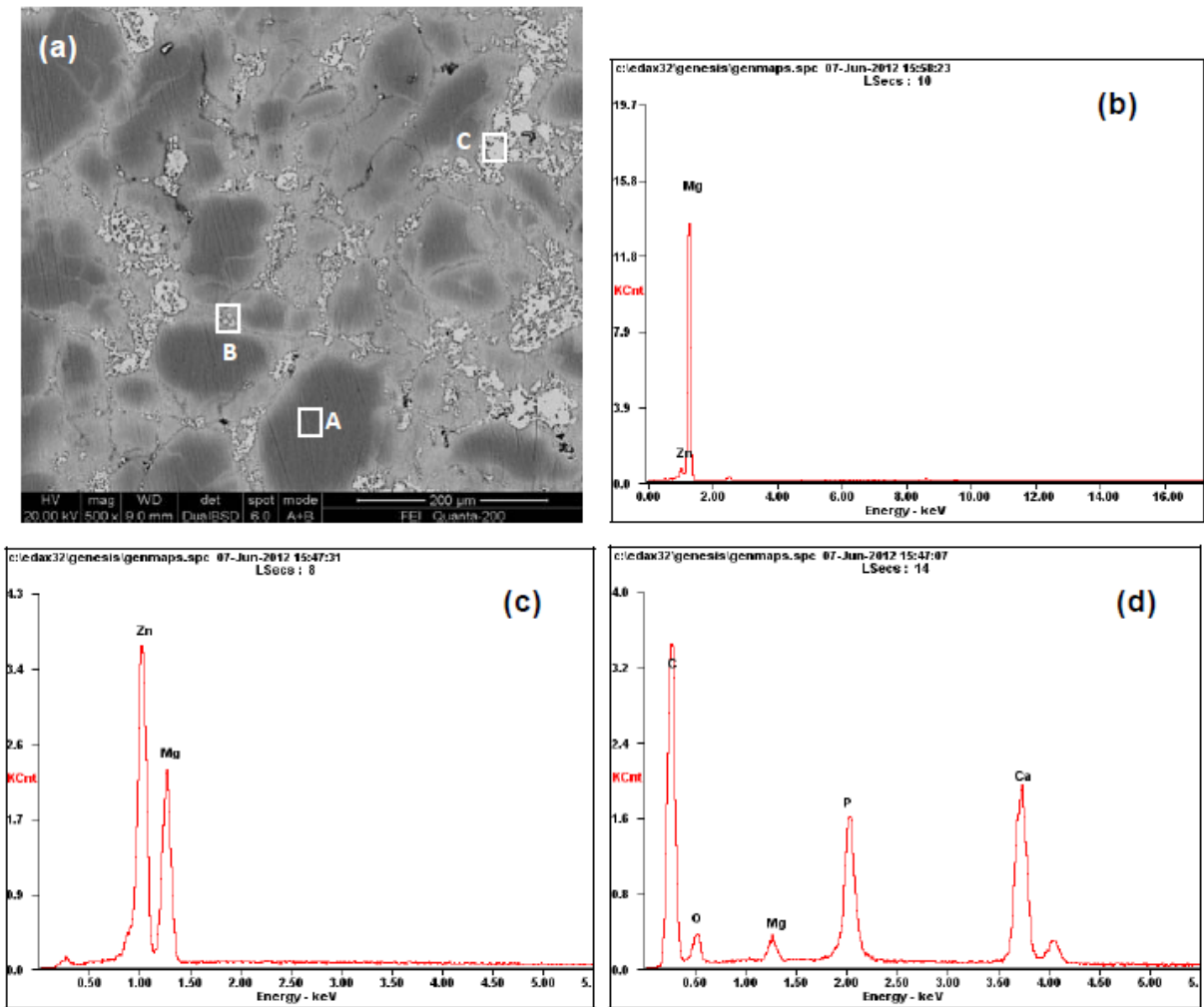


Fig.3

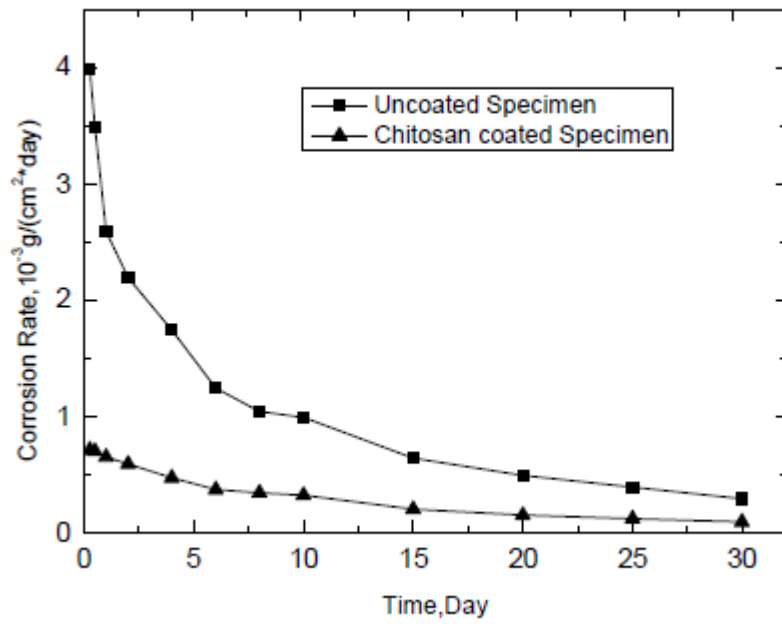


Fig.4

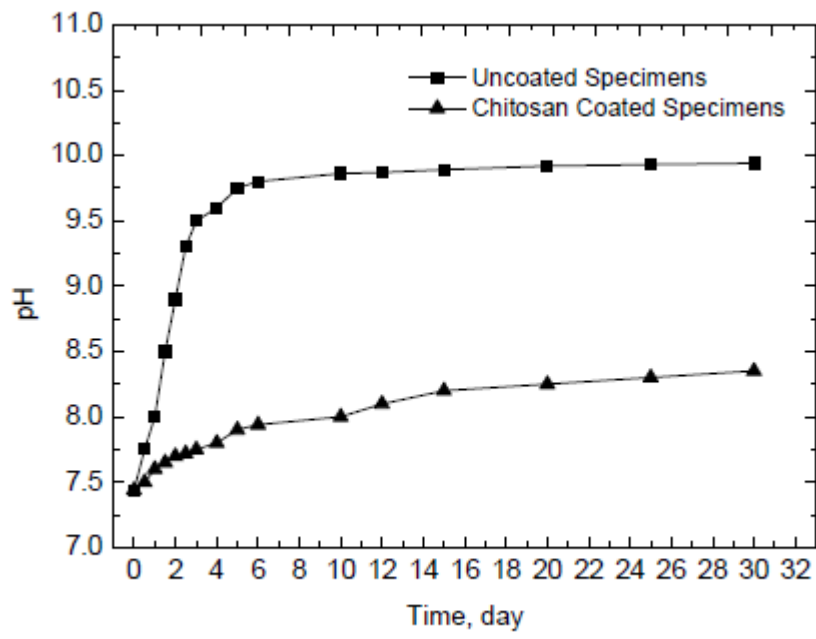


Fig.5

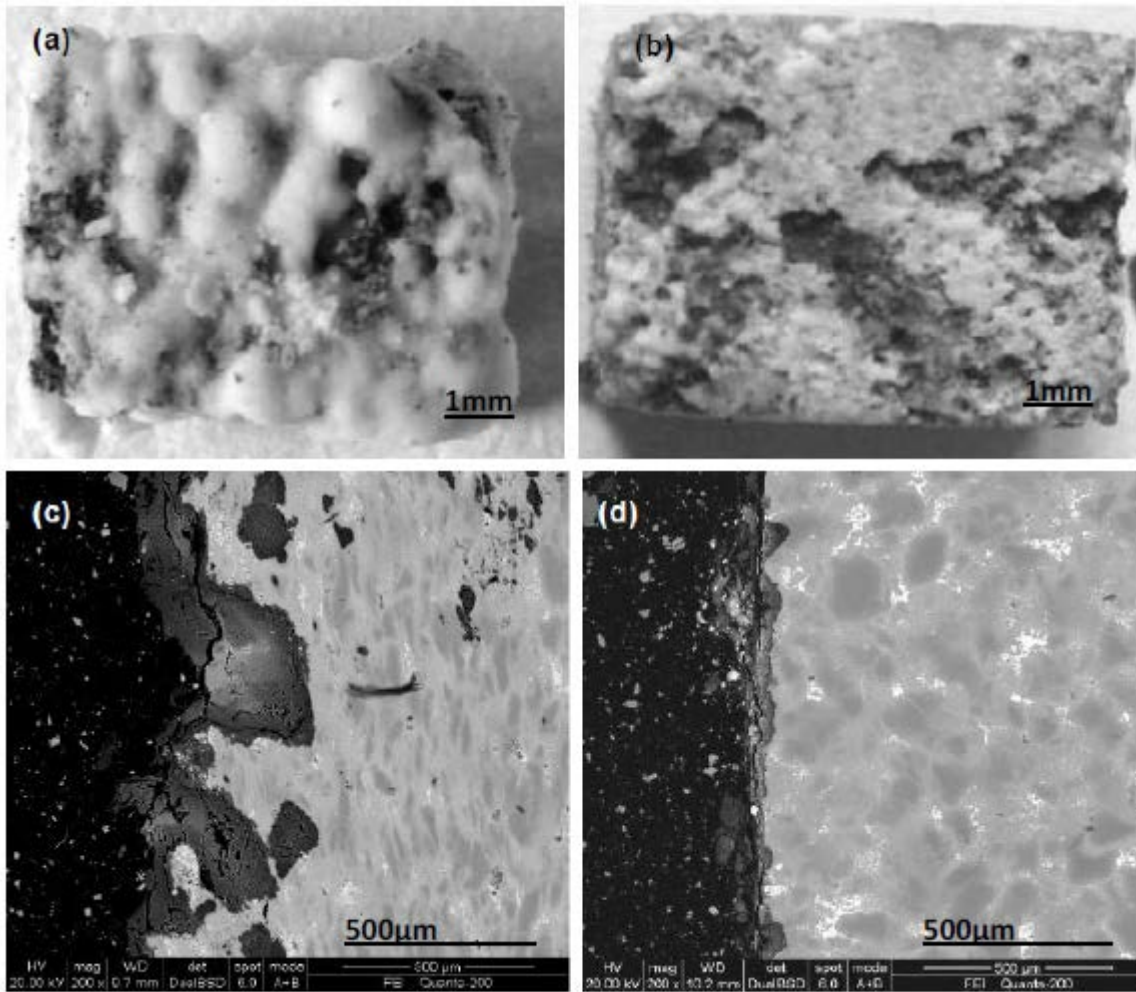


Fig.6

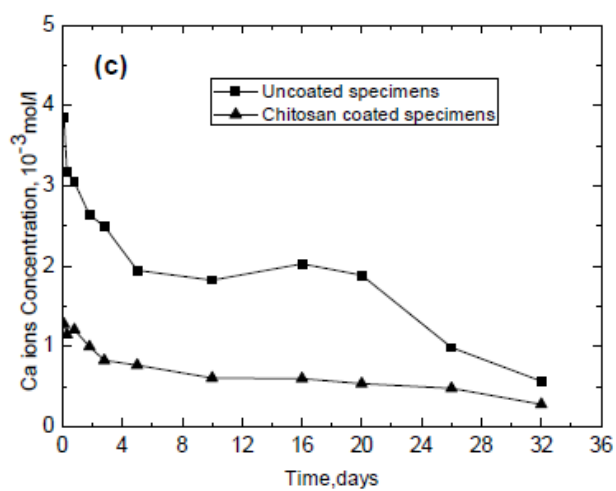
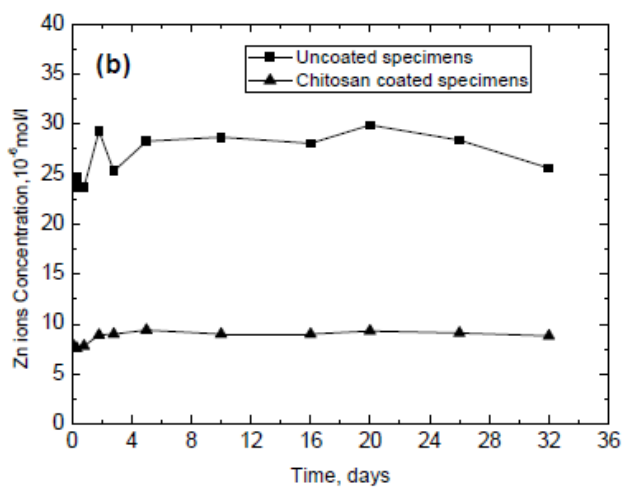
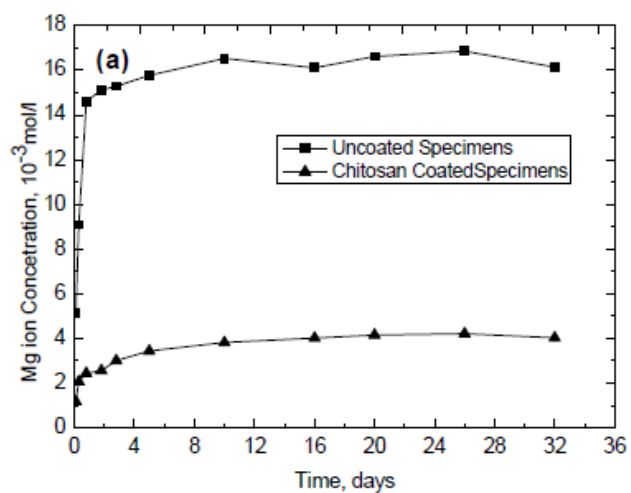


Fig.7

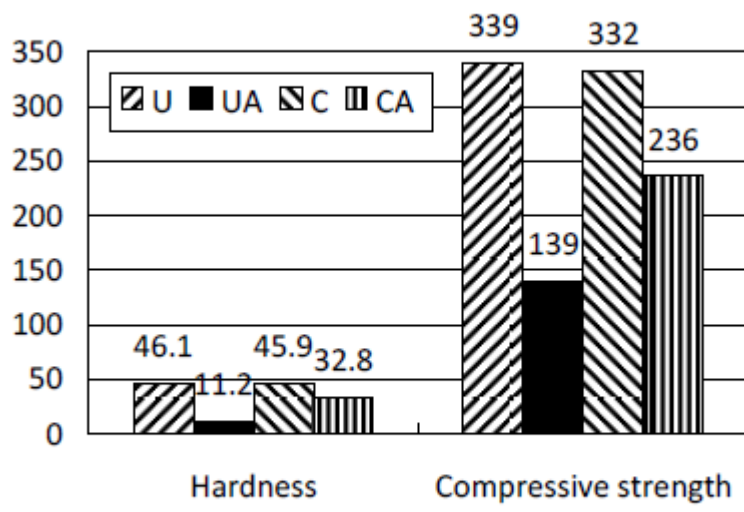


Fig.8

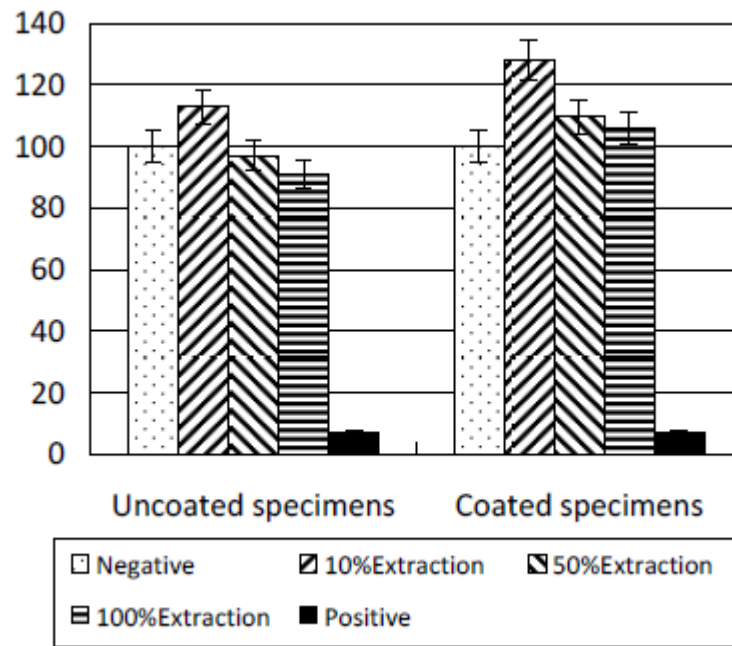


Fig.9

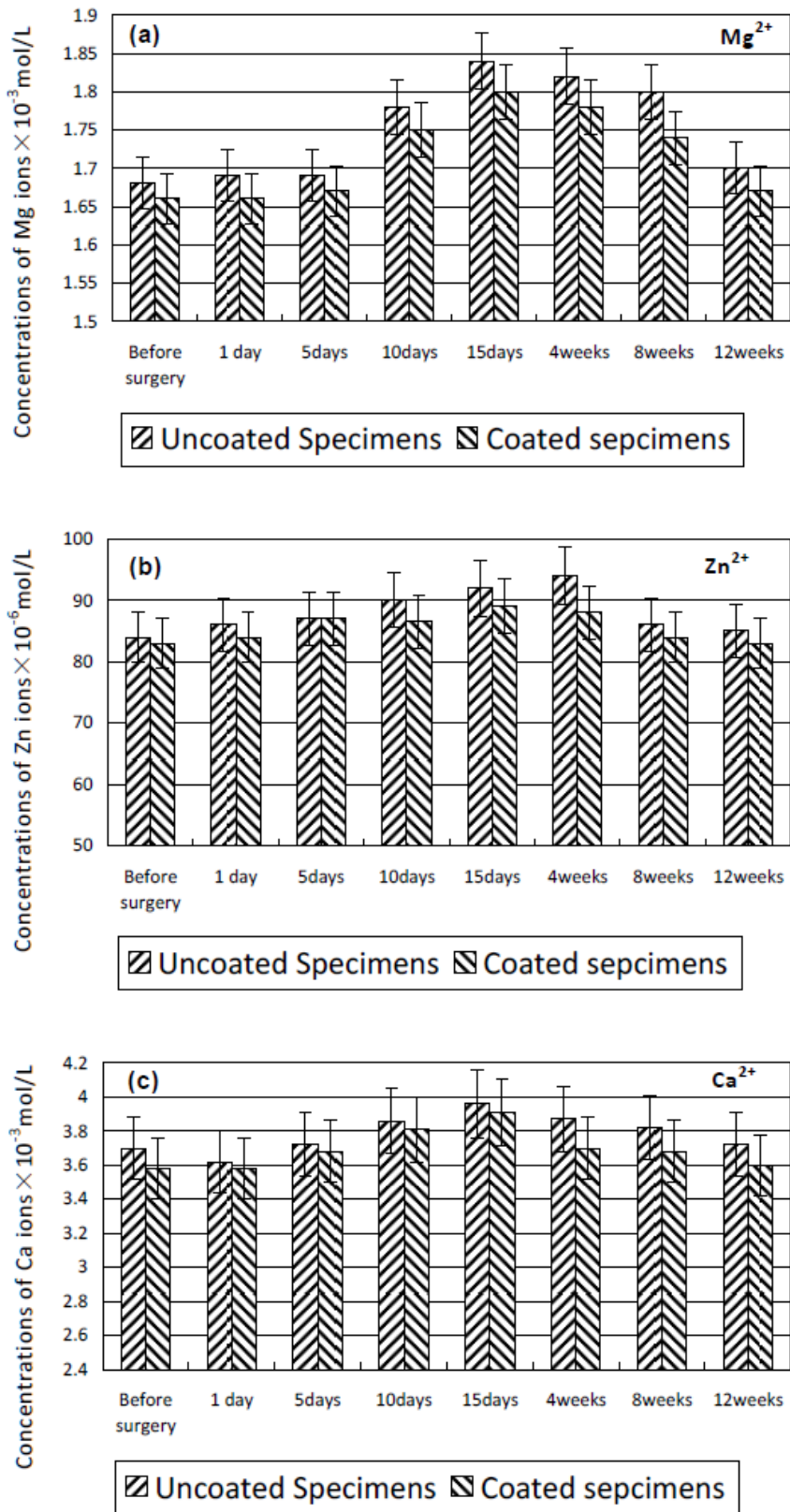


Fig.10

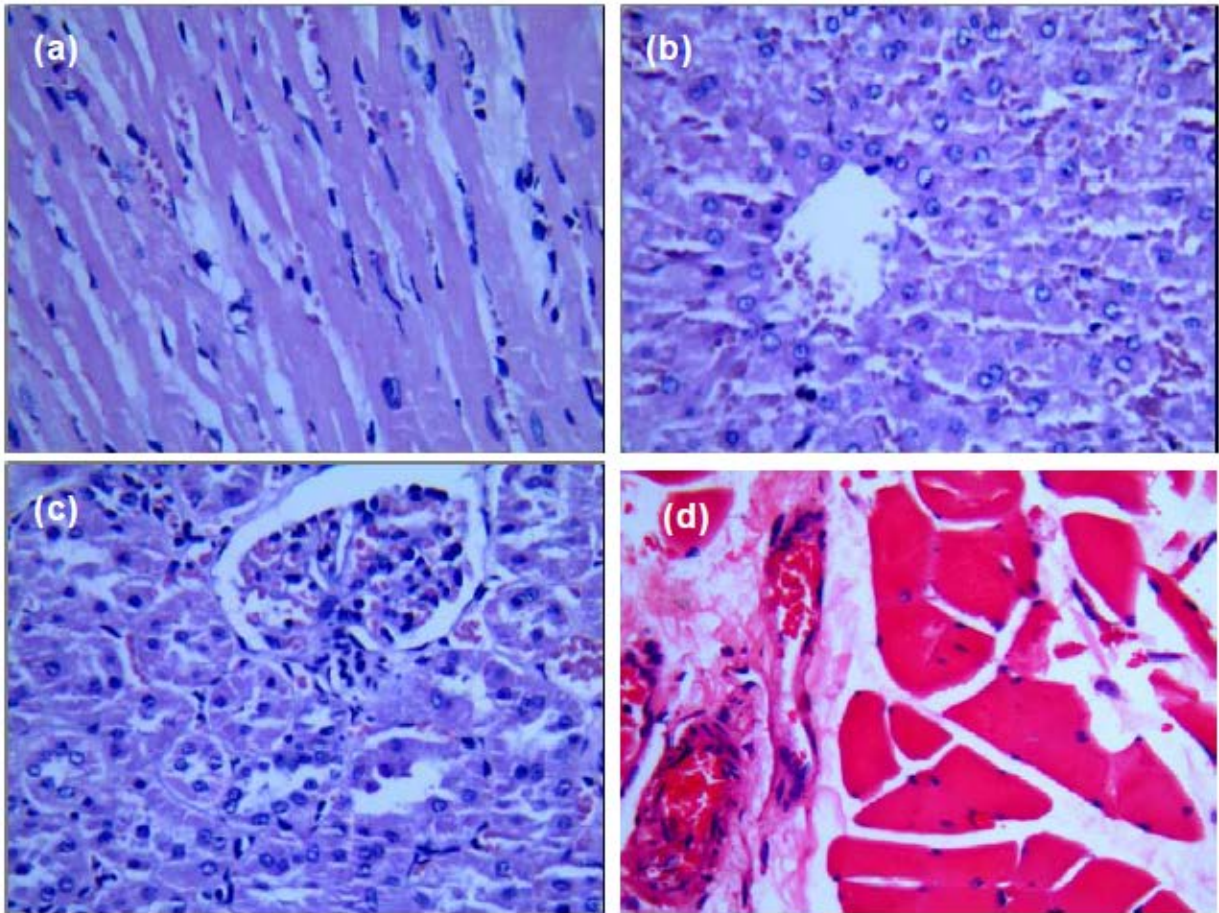


Fig.11

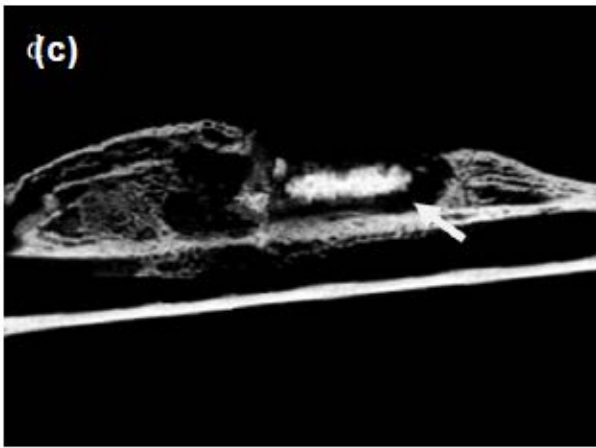
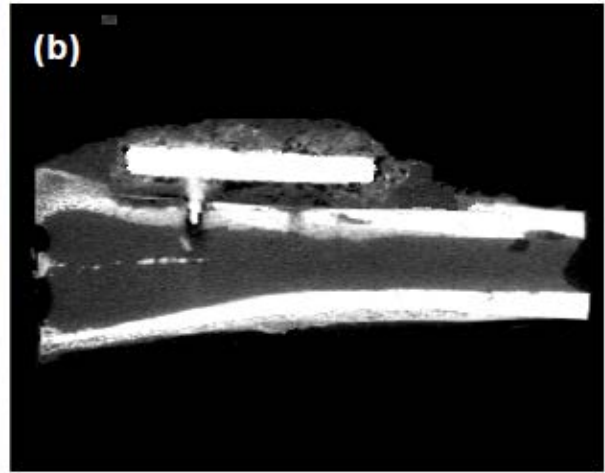
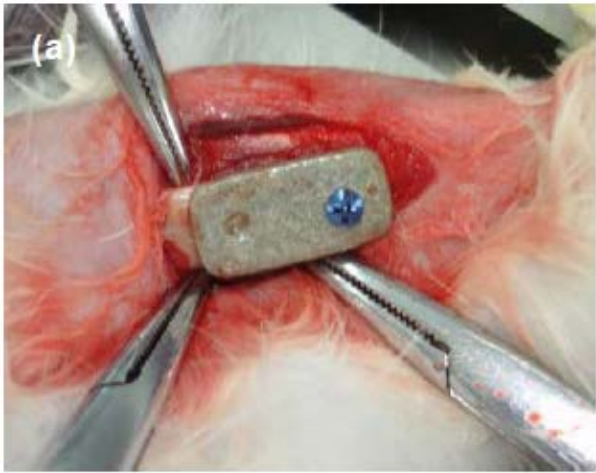


Fig.12

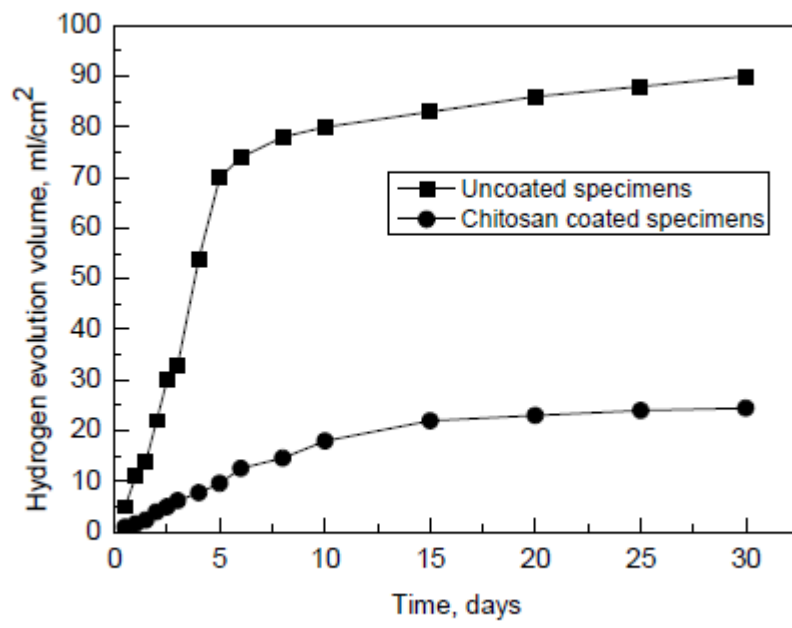


Fig.13

